ANNALS of the ORADEA UNIVERSITY.
Fascicle of Management and Technological Engineering, Volume VI (XVI), 2007

APPLICATION OF VORTEX LATTICE METHODS TO ANALYZE THE PERFORMANCE OF A GLIDER

Robert ENOIU, Georgiana DRAGUSIN
"Transilvania" University of Braşov, Mechanical Engineering,
robertenoiu@yahoo.com, dragusin.georgiana@unitbv.ro

Keywords: Vortex Lattice Method, CFD, glider, horseshoe vortex

Abstract. *This paper presents a method for the calculation of the linear and nonlinear, longitudinal aerodynamics characteristics of various planar shapes including multiple lifting surfaces configurations in subsonic flow at high angle of attack. This method can handle complex platforms such as closely coupled canard-wing combinations, wing-tail combinations, various flaps, elevators, dihedral angles as well as ground effects problems. This method is very easy to use and capable of providing remarkable insight into wing aerodynamics and component interaction. It is the vortex lattice method (vlm), an vas among the earliest methods utilizing computers to actually assist aerodynamicists in estimating aircraft aerodynamics. Vortex lattice methods are based on solution to Laplace`s Equation, and are subject to some basic theoretical restrictions that apply to panel methods.*

1. The Classical Vortex Lattice Method

There are many different vortex lattice schemes. In this paper we describe the "classical" implementation. Knowing that vortices can represent lift from our airfoil analysis, and that one approach is to place the vortex and then satisfy the boundary condition using the "1/4 - 3/4 rules," we proceed as follows:

1) Divide the planform up into a lattice of quadrilateral panels, and put a horseshoe vortex on each panel.
2) Place the bound vortex of the horseshoe vortex on the 1/4 chord element line of each panel.
3) Place the control point on the 3/4 chord point of each panel at the midpoint in the spanwise direction (sometimes the lateral panel centroid location is used) .
4) Assume a flat wake in the usual classical method.
5) Determine the strengths of each Γ_n required to satisfy the boundary conditions by solving a system of linear equations. The implementation is shown schematically in Fig. 1.

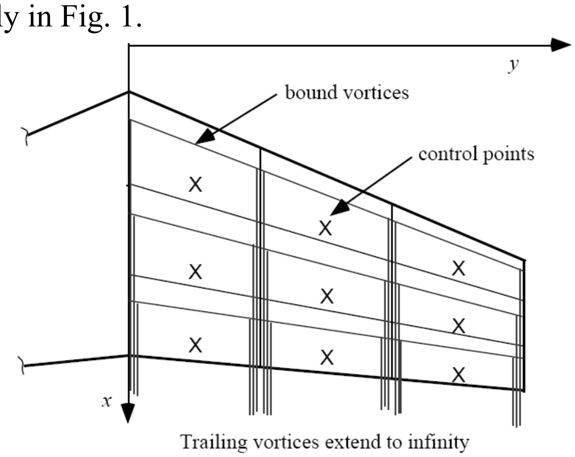

Fig. 1. The horseshoe vortex layout for the classical vortex lattice method.

Note that the lift is on the bound vortices. To understand why, consider the vector statement of the Kutta-Joukowski Theorem, $\mathbf{F} = \rho\mathbf{V} \times\Gamma$. Assuming the freestream velocity is the primary contributor to the velocity, the trailing vortices are parallel to the velocity vector and hence the force on the trailing vortices are zero. More accurate methods find the wake deformation required to eliminate the force in the presence of the complete induced flowfield.

Next, we derive the mathematical statement of the classical vortex lattice method described above. First, recall that the velocity induced by a single horseshoe vortex is:

$$\mathbf{V}_m = \mathbf{C}_{m,n}\Gamma_n. \tag{1}$$

This is the velocity induced at the point m due to the n^{th} horseshoe vortex, where $\mathbf{C}_{m,n}$ is a vector, and the components are given by Equations 2, 3 and 4.

$$\Psi = \frac{\mathbf{r}_1 \times \mathbf{r}_2}{\left|\mathbf{r}_1 \times \mathbf{r}_2\right|^2} = \frac{\left\{\begin{array}{l}\left[(y-y_{1n})(z-z_{2n})-(y-y_{2n})(z-z_{1n})\right]\mathbf{i}\\ -\left[(x-x_{1n})(z-z_{2n})-(x-x_{2n})(z-z_{1n})\right]\mathbf{j}\\ +\left[(x-x_{1n})(y-y_{2n})-(x-x_{2n})(y-y_{1n})\right]\mathbf{k}\end{array}\right\}}{\left\{\begin{array}{l}\left[(y-y_{1n})(z-z_{2n})-(y-y_{2n})(z-z_{1n})\right]^2\\ +\left[(x-x_{1n})(z-z_{2n})-(x-x_{2n})(z-z_{1n})\right]^2\\ +\left[(x-x_{1n})(y-y_{2n})-(x-x_{2n})(y-y_{1n})\right]^2\end{array}\right\}}. \tag{2}$$

$$\mathbf{V}_m = \mathbf{C}_{mn}\Gamma_n \tag{3}$$

$$v_{cp} = -\frac{\Gamma}{2\pi r}. \tag{4}$$

The total induced velocity at m due to the $2N$ vortices (N on each side of the planform) is:

$$\mathbf{V}_{m_{ind}} = u_{m_{ind}}\mathbf{i} + v_{m_{ind}}\mathbf{j} + w_{m_{ind}}\mathbf{k} = \sum_{n=1}^{2N}\mathbf{C}_{m,n}\Gamma_n. \tag{5}$$

The solution requires the satisfaction of the boundary conditions for the total velocity, which is the sum of the induced and freestream velocity. The freestream velocity is (introducing the possibility of considering vehicles at combined angle of attack and sideslip):

$$\mathbf{V}_\infty = V_\infty\cos\alpha\cos\beta\,\mathbf{i} - V_\infty\sin\beta\,\mathbf{j} + V_\infty\sin\alpha\cos\beta\,\mathbf{k} \tag{6}$$

so that the total velocity at point *m* is:

$$\mathbf{V}_m = (V_\infty \cos\alpha \cos\beta + u_{m_{ind}})\,\mathbf{i} + \left(-V_\infty \sin\beta + v_{m_{ind}}\right)\mathbf{j} + (V_\infty \sin\alpha \cos\beta + w_{m_{ind}})\,\mathbf{k}\,\cdot \tag{7}$$

The values of the unknown circulations, Γ_n, are found by satisfying the non-penetration boundary condition at all the control points simultaneously. For steady flow this is:

$$\mathbf{V}\cdot\mathbf{n} = 0 \tag{8}$$

where the surface is described by:

$$F(x,y,z) = 0\,. \tag{9}$$

Equation (8) can then be written:

$$\mathbf{V}\cdot\frac{\nabla F}{|\nabla F|} = \mathbf{V}\cdot\nabla F = 0\,. \tag{10}$$

This equation provides freedom to express the surface in a number of forms. The most general form is obtained by substituting Eqn. (7) into Eqn. (9) using Eqn. (5). This can be written as:

$$\left[(V_\infty \cos\alpha \cos\beta + u_{m_{ind}})\,\mathbf{i} + \left(-V_\infty \sin\beta + v_{m_{ind}}\right)\mathbf{j} + (V_\infty \sin\alpha \cos\beta + w_{m_{ind}})\,\mathbf{k}\right]\cdot \left[\frac{\partial F}{\partial x}\mathbf{i} + \frac{\partial F}{\partial y}\mathbf{j} + \frac{\partial F}{\partial z}\mathbf{k}\right] = 0 \tag{11}$$

or,

$$\left[(V_\infty \cos\alpha \cos\beta + \sum_{n=1}^{2N} C_{m,n_\mathbf{i}}\Gamma_n)\,\mathbf{i} + \left(-V_\infty \sin\beta + \sum_{n=1}^{2N} C_{m,n_\mathbf{j}}\Gamma_n\right)\mathbf{j} + (V_\infty \sin\alpha \cos\beta + \sum_{n=1}^{2N} C_{m,n_\mathbf{k}}\Gamma_n)\,\mathbf{k}\right]\cdot \left[\frac{\partial F}{\partial x}\mathbf{i} + \frac{\partial F}{\partial y}\mathbf{j} + \frac{\partial F}{\partial z}\mathbf{k}\right] = 0 \tag{12}$$

Carrying out the dot product operation and collecting terms:

$$\frac{\partial F}{\partial x}(V_\infty \cos\alpha \cos\beta + \sum_{n=1}^{2N} C_{m,n_\mathbf{i}}\Gamma_n) + \frac{\partial F}{\partial y}\left(-V_\infty \sin\beta + \sum_{n=1}^{2N} C_{m,n_\mathbf{j}}\Gamma_n\right) + \frac{\partial F}{\partial z}(V_\infty \sin\alpha \cos\beta + \sum_{n=1}^{2N} C_{m,n_\mathbf{k}}\Gamma_n) = 0\,\cdot \tag{13}$$

Recall that Eqn. (13) is applied to the boundary condition at point *m*. Next step is to collect terms to clearly identify the expression for the circulation. The resulting expression defines a system of equations for all the panels, and is the system of linear algebraic equations that is used to solve for the unknown values of the circulation distribution. The result is:

$$\sum_{n=1}^{2N}\left(\frac{\partial F}{\partial x}C_{m,n_\mathbf{i}} + \frac{\partial F}{\partial y}C_{m,n_\mathbf{j}} + \frac{\partial F}{\partial z}C_{m,n_\mathbf{k}}\right)\Gamma_n = -V_\infty\left[\cos\alpha\cos\beta\frac{\partial F}{\partial x} - \sin\beta\frac{\partial F}{\partial y} + \sin\alpha\cos\beta\frac{\partial F}{\partial z}\right]$$

$$m=1,\ldots 2N \tag{14}$$

This is the general equation used to solve for the values of the circulation. It is arbitrary, containing effects of both angle of attack and sideslip (if the vehicle is at sideslip the trailing vortex system should by yawed to align it with the freestream).

If the surface is primarily in the *x-y* plane and the sideslip is zero, we can write a simpler form. In this case the natural description of the surface is:

$$z = f(x, y) \tag{15}$$

and

$$F(x, y, z) = z - f(x, y) = 0\,. \tag{16}$$

The gradient of *F* becomes

$$\frac{\partial F}{\partial x} = -\frac{\partial f}{\partial x},\quad \frac{\partial F}{\partial y} = -\frac{\partial f}{\partial y},\quad \frac{\partial F}{\partial z} = 1\cdot \tag{17}$$

Substituting into the statement of the boundary condition, Eqn. (14), we obtain:

$$\sum_{n=1}^{2N}\left[C_{m,n\,\mathbf{k}} - \frac{\partial f}{\partial x}C_{m,n\,\mathbf{i}} - \frac{\partial f}{\partial y}C_{m\,n\,\mathbf{j}}\right]\Gamma_n = V_\infty\left(\cos\alpha\,\frac{\partial f}{\partial x} - \sin\alpha\right),\qquad m = 1,\ldots,2N\cdot \tag{18}$$

This equation provides the solution for the vortex lattice problem.

To illustrate the usual method, consider the simple planar surface case, where there is no dihedral. Furthermore, recalling the example in the last section and the analysis at the beginning of the chapter, the thin airfoil theory boundary conditions can be applied on the mean surface, and not the actual camber surface. We also use the small angle approximations. Under these circumstances, Eqn. (18) becomes:

$$w_m = \sum_{n=1}^{2N} C_{m\,n\mathbf{k}}\,\Gamma_n = V_\infty\left(\frac{df_c}{dx} - \alpha\right)\Bigg|_m\,. \tag{19}$$

Thus we have the following equation which satisfies the boundary conditions and can be used to relate the circulation distribution and the wing camber and angle of attack:

$$\sum_{n=1}^{2N} C_{m,n\mathbf{k}}\left(\frac{\Gamma_n}{V_\infty}\right) = \left(\frac{df_c}{dx} - \alpha\right)_m \qquad m = 1,\ldots,2N\cdot \tag{20}$$

Equation (20) contains two cases:

1) *The Analysis Problem*. Given camber slopes and α, solve for the circulation strengths, $(\Gamma/V\infty)$ [a system of $2N$ simultaneous linear equations].

or

2) *The Design Problem*. Given $(\Gamma/V\infty)$, which corresponds to a specified surface loading, we want to find the camber and α required to generate this loading (only requires simple algebra, no system of equations must be solved).

Notice that the way d*f*c/d*x* and α are combined illustrates that the division between camber, angle of attack and wing twist is arbitrary (twist can be considered a separate part of the camber distribution, and is useful for wing design). However, care must be taken in keeping the bookkeeping straight.

One reduction in the size of the problem is available in many cases. If the geometry is symmetrical and the camber and twist are also symmetrical, then Γ_n is the same on each side of the planform (but *not* the influence coefficient). Therefore, we only need to solve for N Γ's, not $2N$ (this is true also if ground effects are desired, see Katz and Plotkin[1]). The system of equations for this case becomes:

$$\sum_{n=1}^{N}\left[C_{m,n\mathbf{k}\,\mathrm{left}} + C_{m,n\mathbf{k}\,\mathrm{right}}\right]\left(\frac{\Gamma_n}{V_\infty}\right) = \left(\frac{df_c}{dx} - \alpha\right)_m \qquad m = 1,\ldots,N\,. \tag{21}$$

This is easy. Why not just program it up ourselves? You can, but most of the work is:

A. Automatic layout of panels for arbitrary geometry. As an example, when considering multiple lifting surfaces, the horseshoe vortices on each surface must "line up". The downstream leg of a horseshoe vortex cannot pass through the control point of another panel.

and

B. Converting Γn to the aerodynamics values of interest, C_L, C_m, *etc*., and the spanload, is tedious for arbitrary configurations.

Nevertheless, many people (including previous students in the Applied Computational Aerodynamics class) have written **vlm** codes. The method is widely used in industry and government for aerodynamic estimates for conceptual and preliminary design predictions. The method provides good insight into the aerodynamics of wings, including interactions between lifting surfaces.

Typical analysis uses (in a design environment) include:

- ♦ Predicting the configuration neutral point during initial configuration layout, and studying the effects of wing placement and canard and/or tail size and location.
- ♦ Finding the induced drag, C_{Di}, from the spanload in conjunction with farfield methods.
- ♦ • With care, estimating control and device deflection effectiveness (estimates where viscous effects may be important require calibration. Some examples are shown in the next section. For example, take 60% of the inviscid value to account for viscous losses, and also realize that a deflection of $\delta f = 20 - 25°$ is about the maximum useful device deflection in practice).
- ♦ Investigating the aerodynamics of interacting surfaces.
- ♦ Finding the lift curve slope, $C_{L\alpha}$, approach angle of attack, *etc*.

Typical design applications include:

- ♦ Initial estimates of twist to obtain a desired spanload, or root bending moment.
- ♦ Starting point for finding a camber distribution in purely subsonic cases.

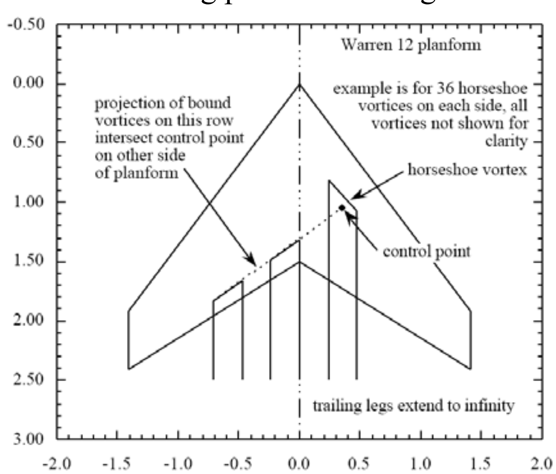

Figre.2.
Example of case requiring special treatment, the intersection of the projection of a vortex with a control point.

Before examining how well the method works, two special cases require comments. The first case arises when a control point is in line with the projection of one of the finite length vortex segments. This problem occurs when the projection of a swept bound vortex segment from one side of the wing intersects a control point on the other side. This happens frequently. The velocity induced by this vortex is zero, but the equation as usually written degenerates into a singular form, with the denominator going to zero. Thus a special form should be used. In practice, when this happens the contribution can be set to zero without invoking the special form. Figure 2 shows how this happens. Using the Warren 12 planform and 36 vortices on each side of the wing, we see that the projection of the line of bound vortices on the last row of the left hand side of the planform has a projection that intersects one of the control points on the right hand side.

A model problem illustrating this can be constructed for a simple finite length vortex segment. The velocity induced by this vortex is shown in Fig. 3. When the vortex is approached directly, x/l = 0.5, the velocity is singular for h = 0. However, as soon as you approach the axis (h = 0) off the end of the segment (x/l > 1.0) the induced velocity is zero. This illustrates why you can set the induced velocity to zero when this happens.

This second case that needs to be discussed arises when two or more planforms are used with this method. This is one of the most powerful applications of the vortex lattice method. However, care must be taken to make sure that the trailing vortices from the first surface do not intersect the control points on the second surface. In this case the induced velocity is in fact infinite, and the method breaks down. Usually this problem is solved by using the same spanwise distribution of horseshoe vortices on each surface. This aligns the vortex the legs, and the control points are well removed from the trailing vortices of the forward surfaces.

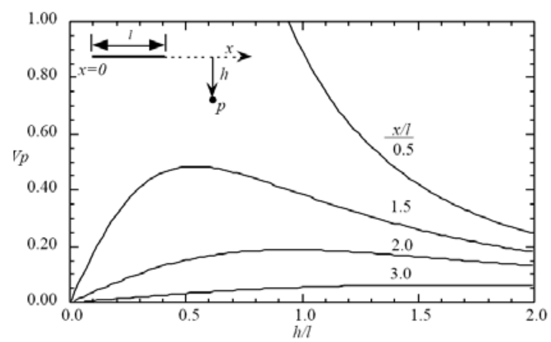

Figure 3. Velocity induced by finite straight line section of a vortex.

2. Examples of the Use and Accuracy of the vlm Method

The vortex lattice layout is clear for most wings and wing-tail or wing-canard configurations. The method can be used for wing-body cases by simply specifying the projected planform of the entire configuration as a flat lifting surface made up of a number of straight line segments. The exact origin of this somewhat surprising approach is unknown. The success of this approach is illustrated in examples given below.

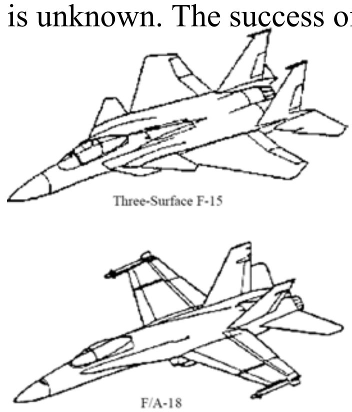

Fig. 4. Configurations used by McDonnell Aircraft to study **vlm** method accuracy

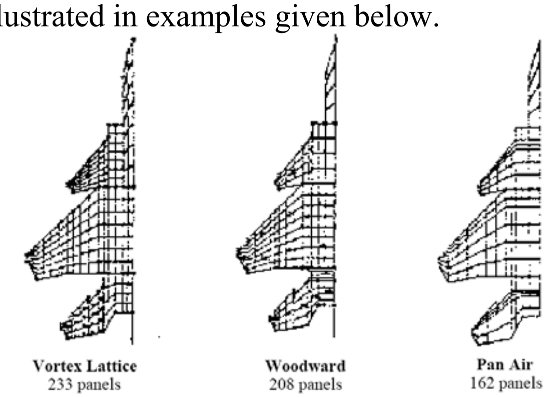

Fig. 5. Panel models used for the three-surface F-15

Aircraft configurations examined by John Koegler [10]

As part of a study on control system design methods, John Koegler at McDonnell Aircraft Company studied the prediction accuracy of several methods for fighter airplanes. In addition to the vortex lattice method, he also used the PAN AIR and Woodward II panel methods. He compared his predictions with the three-surface F-15, which became known as the STOL/Maneuver demonstrator, and the F-18. These configurations are illustrated in Fig. 4.

Considering the F-15 STOL/Maneuver demonstrator first, the basic panel layout is given in Figure 5. This shows how the aircraft was modeled as a flat planform, and the corner points of the projected configuration were used to represent the shape in the vortex lattice method and the panel methods. Note that in this case the rake of the wingtip was included in the computational model. In this study the panel methods were also used in a purely planar surface mode. In the vortex lattice model the configuration was divided into three separate planforms, with divisions at the wing root leading and trailing edges. On this configuration each surface was at a different height and, after some experimentation, the vertical distribution of surfaces shown in Figure 6 was found to provide the best agreement with wind tunnel data.

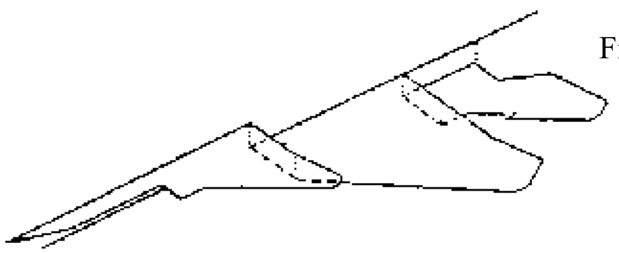

Fig. 6. Canard and horizontal tail height representation

The results from these models are compared with wind tunnel data in Table 1. The vortex lattice method is seen to produce excellent agreement with the data for the neutral point location, and lift and moment curve slopes at Mach 0.2.

Subsonic Mach number effects are simulated in **vlm** methods by transforming the Prandtl-Glauert equation which describes the linearized subsonic flow to Laplace's Equation using the Göthert transformation. However, this is only approximately correct and the agreement with wind tunnel data is not as good at the transonic Mach number of 0.8. Nevertheless, the **vlm** method is as good as PAN AIR used in this manner. The **vlm** method is not applicable at supersonic speeds. The wind tunnel data shows the shift in the neutral point between subsonic and supersonic flow. The Woodward method, as applied here, over predicted the shift with Mach number. Note that the three-surface configuration is neutral to slightly unstable subsonically, and becomes stable at supersonic speeds.

Table 1. Three-Surface F-15 Longitudinal Derivatives

Data Source		Neutral Point (% mac)	$C_{m\alpha}$ (1/deg)	$C_{L\alpha}$ (1/deg)
M = 0.2	Wind Tunnel	15.70	.00623	.0670
	Vortex Lattice	15.42	.00638	.0666
	Woodward	14.18	.00722	.0667
	Pan Air	15.50	.00627	.0660
M = 0.8	Wind Tunnel	17.70	.00584	.0800
	Vortex Lattice	16.76	.00618	.0750
	Pan Air	15.30	.00684	.0705
M = 1.6	Wind Tunnel	40.80	-.01040	.0660
	Woodward	48.39	-.01636	.0700

3. Results obtain using the VLM method for the IS29D2 glider

For determining the best configuration of horseshoe vortices to be used on the model we have tested different tips of mashes starting with 4 horseshoe vortices chordwise in combination with 12 horseshoe vortices spanwise and ending with 6 horseshoe vortices chordwise in combination with 20 horseshoe vortices spanwise. The best solution is, as you can see in figure 7, the one with 6 horseshoe vortices chordwise in combination with 20 horseshoe vortices spanwise.

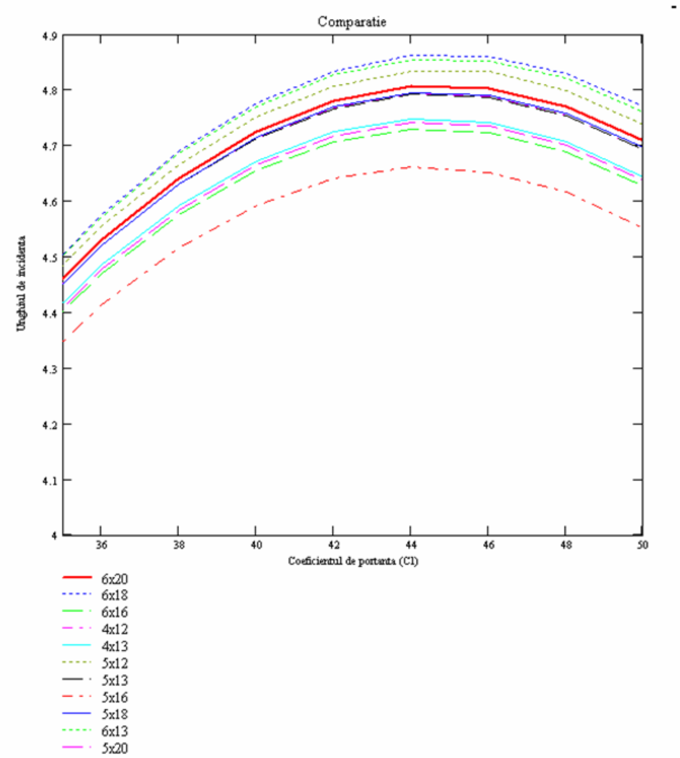

Figure 6. Configuration of horseshoe vortices

The result obtain using the chosen configuration are presented in the figure 7 to 17.

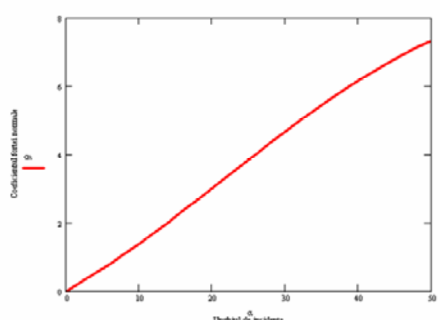

Fig.7. Cn/α

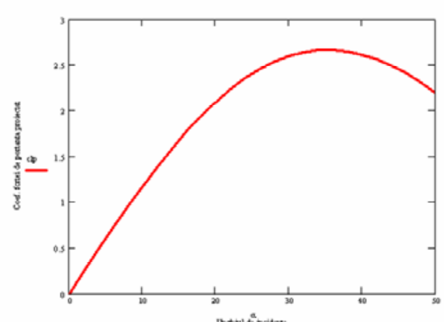

Fig.8. Clp/α

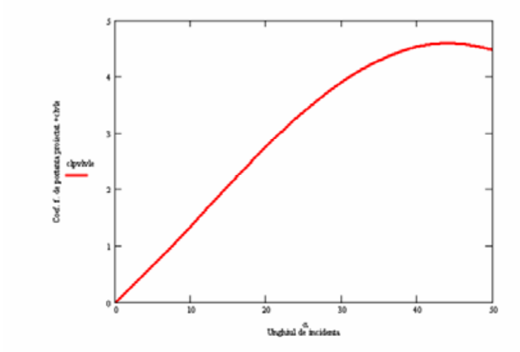

Fig.9. Clp+vlvle/α

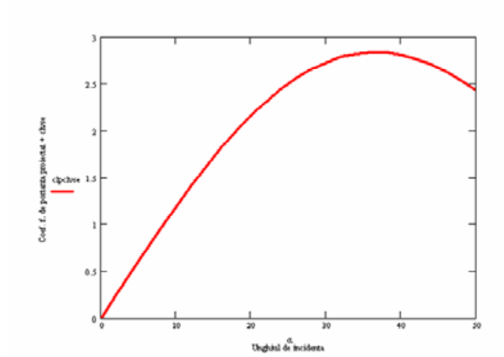

Fig.10. Clp+clvse/α

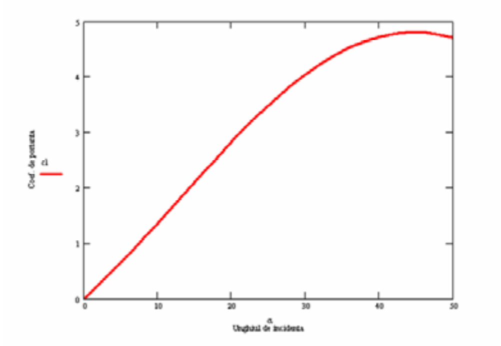

Fig.11. Cl/α

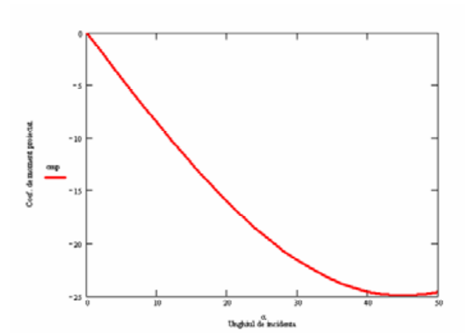

Fig.12. Cmp/α

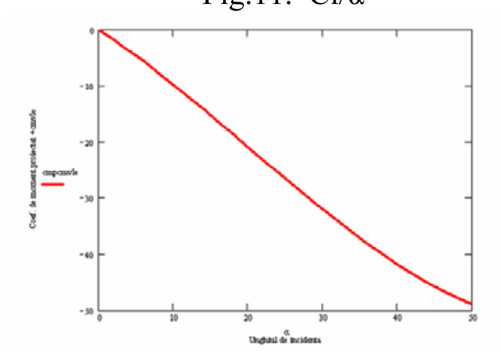

Fig.13. Cmpcmvle/α

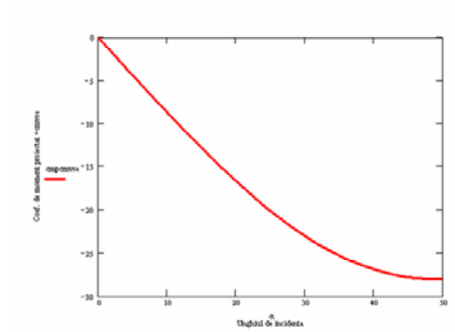

Fig.14. Cmpcmvse/α

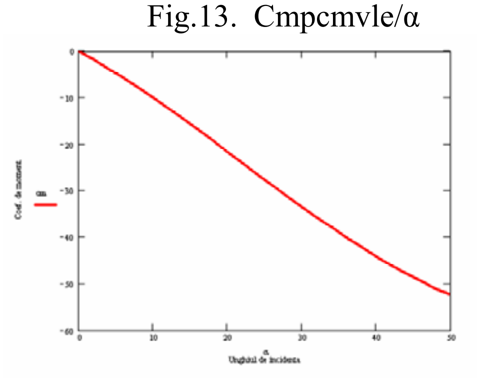

Fig.15. Cm/α

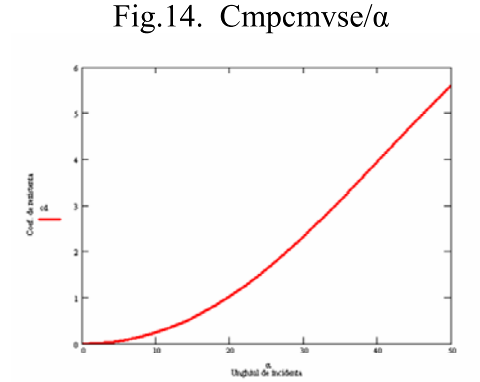

Fig.16. Cd/α

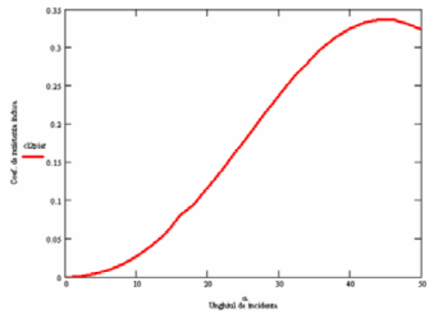

Fig.17. Cl**2pi*ar/α

Where:

- Cl – lift coefficient
- Clp – projected lift coefficient
- Cd – drag coefficient
- Cm – moment coefficient
- Cmp – projected moment coefficient
- α – angle of attack

References

1. *W. H. Mason, mason@aoe.vt.edu*
2. *Rubbert, P. E. "Theoretical Characteristics of Arbitrary Wings by a Non-Planar Vortex Latice Method" 1964 The Boeing Co., Seattle, Wash.*
3. *Dulmovist, J., "A Lifting Surface Method for Calculating Load Distribution and the Aerodynamic Influence Coefficient Matrix for Wing in Subsonic Flow" 1964, Grumman Aircraft Engineering Corp., Bethpage , N.Y.*
4. *Hedman, S. G., "Vortex Lattice Method for Calculation of Quasi Steady State Loadings on Thin Elastic Wings," Oct. 1965 Aeronautical Research Institute of Sweden, Sweden*
5. *Belotserkovskii, S. M., "The Theory of Thin Wings in Subsonic Flow: 1967, N.Y.*
6. *Margason, R.J., and Lamar, J.E., "Vortex-Lattice FORTRAN Program for Estimating Subsonic Aerodynamic Characteristics of Complex Planforms," NASA TN D-6142, Feb., 1971.*
7. *Lamar, J.E., and Gloss, B. B. "Subsonic Aerodynamic Characteristics of Interacting Lifting Surfaces with Separated Flow around Sharp Edges Predicted by a Vortex-Lattice Method," NASA TN D-7921, Sept., 1975.*
8. *Lamar, J.E., and Frink, N.T., "Experimental and Analytic Study of the Longitudinal AerodynamicCharacteristics of Analytically and Empirically Designed Strake-Wing Configurations at Subcritical Speeds, " NASA TP-1803, June 1981.*
9. *Lamar, J.E., and Herbert, H.E., "Production Version of the Extended NASA-Langley Vortex Lattice FORTRAN Computer Code," - Vol. I - User's Guide, NASA TM 83303, April 1982.*
10. *Thomas, R.W., "Analysis of Aircraft Stability and Control Design Methods," AFWAL-TR-84-3038, Vol. II, App. B., "Evaluation of Aerodynamic Panel Methods," by John Koegler, May,1984.*
11. *Katz, J., and Plotkin, A., Low-Speed Aerodynamics: From Wing Theory to Panel Methods, McGraw-Hill, Inc., New York, 1991.*